JOURNAL OF APPLIED ELECTROCHEMISTRY 22 (1992) 711–716

Preparation and properties of Raney nickel electrodes on Ni–Zn base for H_2 and O_2 evolution from alkaline solutions Part II: Leaching (activation) of the Ni–Zn electrodeposits in concentrated KOH solutions and H_2 and O_2 overvoltage on activated Ni–Zn Raney electrodes

J. BALEJ*

Consultant Bureau for Chemical Engineering, Teichstrasse 9, D-5170 Jülich, Germany

J. DIVISEK, H. SCHMITZ, J. MERGEL

Research Centre (KFA) Jülich, Institute of Applied Physical Chemistry, P.O. Box 1913, D-5170 Jülich, Germany

Received 25 June 1991; revised 14 December 1991

The partial dissolution of zinc from electrodeposited Ni–Zn alloys (with X^0_{Zn} = 22–87.3 mol %) was studied in cold and nearly boiling 10 M KOH. It was found that alloys with $X^0_{Zn} \leqslant 22$ mol % are not dissolved at all. The dissolved zinc fraction, A, increased rapidly with further increase in zinc content and after having passed a maximum with A = 82–90% at X^0_{Zn} = 55–58 mol % and a sharp minimum with A = 52–65% at X^0_{Zn} = 65–69 mol %, it asymptotically approached to $A \rightarrow 100\%$ at $X^0_{Zn} \rightarrow 100$ mol %. The discontinuous dependence of A against X^0_{Zn} may be explained by differences in the crystallographic composition of the alloy deposits. Alloys with $X^0_{Zn} < 50$–60 mol % can be allocated to solid solutions of zinc in the Ni matrix (α-phase); the range of 50–60 $< X^0_{Zn} <$ 70–80 mol % corresponds to the coexistence of $\alpha + \gamma$ phases. The pure γ-phase exists within a narrow range at X^0_{Zn} = 75–80 mol %. No zinc dissolution from Ni–Zn alloys with $X^0_{Zn} \leqslant 22$ mol % was explained by extremely low zinc activities in dilute solid solutions of the α-phases shifting the Gibbs energy of the dissolution reaction to very low negative, or even to positive values. The dependence of the hydrogen and oxygen overvoltage at $j = 0.4\,A\,cm^{-2}$ in 10 M KOH at 100° C on the original zinc content X^0_{Zn} showed, in both cases, a clear minimum at X^0_{Zn} = 75–78 mol %. This points to a practically pure γ-phase in the original Ni–Zn alloy with an approximate composition $NiZn_3$.

1. Introduction

In a preceding study [1] the composition of Ni–Zn alloys electrodeposited from chloride solutions (with about 30 g dm^{-3} H_3BO_3, without further additions) was investigated as a function of different operating conditions (current density, solution composition and pH, temperature, flow rate). The aim was to determine suitable conditions for the electrodeposition of these alloys of optimum composition as precursors of highly active Raney nickel electrodes for hydrogen and oxygen evolution from alkaline solutions.

In the first part of this paper, results of investigations of the selective zinc dissolution from electrodeposited Ni–Zn alloys in approximately 10 M KOH as a function of the original alloy composition are presented. Studies of this type have not been previously described, although the analogous activation of Raney nickel based on Ni–Al has been studied extensively (for example, see [2]). In order to obtain some information about the phase composition of the original (unleached) Ni–Zn alloys, some orientation measurements of the rest potentials of these alloys were carried out.

The second part of this paper provides results of hydrogen and oxygen overvoltage measurements in 10 M KOH at 100° C and ambient pressure on Raney nickel electrodes on activated Ni–Zn base. Little attention has been paid so far in the literature to this problem [3, 4]. Furthermore, it should be noted that the Ni–Zn alloys used in those investigations were

* Present address: Johanniterstrasse 28, D-8850 Donauwörth, Germany.

0021-891X/92

prepared in a different manner from those used in this work.

2. Experimental details

2.1. *Leaching (activation)*

Visually homogeneous samples (approximately 1 cm × 1 cm) of Ni–Zn alloys deposited on perforated Ni sheet [1] were immersed in 100 cm^3 10 M KOH in a beaker (DURAN, Schott) at room temperature. In most cases, intensive hydrogen evolution due to the spontaneous selective dissolution of zinc began either immediately or after various startup times, as follows:

$$Zn + 2OH^- + 2H_2O \longrightarrow Zn(OH)_4^{2-} + H_2 \quad (1)$$

Hydrogen evolution ceased completely after a certain time (a few hours at the most); the temperature was then gradually increased almost up to the boiling point of the solution (approximately 120° C) which resulted in a continuation of zinc dissolution with hydrogen evolution. After this second phase of activation, the samples were taken out of the KOH solution and boiled several times with deionized water. The leached alloy coating was mechanically removed from a small fraction of the sample and used for chemical analysis according to the process described in [1]. The remaining part of the leached samples was preserved in deionized water for further investigations of hydrogen and oxygen overvoltage.

Rest potentials of samples (1 cm × 1 cm) of the original (nonactivated) Ni–Zn alloys against a reference electrode of pure electrodeposited zinc (99.95%) were measured in the cell

$$Ni\text{–}Zn(X_{Zn}^0)|(1M\ ZnSO_4 + 1\,M\ ZnCl_2)|Zn \quad (2)$$

in a thermostatted glass vessel (DURAN) at 25 or 40° C. No mechanical renewal of the alloy surface, as in a similar measurement with thermal Ni–Zn alloys [7], was applied.

2.2. *Hydrogen and oxygen overvoltage*

Measurements of the hydrogen and oxygen overvoltage during water electrolysis from 10 M KOH at 100 ± 1° C and ambient pressure were carried out in closed electrolysis vessels made of PTFE, as already described elsewhere [5, 6]. Five such vessels operated simultaneously. The electrode specimens (1 cm × 1 cm) with previously activated electrodeposited Ni–Zn layers of known original composition were equipped with a nickel wire lead (diam. 2 mm) insulated with PTFE. An Hg/HgO (10 M KOH) reference electrode, kept at room temperature, was immersed in the electrolysis vessel shortly before measuring the steady-state polarization curve in the range 0.1–1.0 A cm^{-2}. Before measurements, the electrode was cathodically or anodically loaded for at least 24 h at a constant current density, $j = 0.4$ A cm^{-2}.

In order to avoid any possible influence on the catalytic activity of the cathode by anodic prepolarization, the cathodic hydrogen overvoltage was measured first for each electrode and only after this was the anodic oxygen overvoltage measured. The *IR*-free potential difference E_c or E_a was measured by means of the interruption method with the aid of a circuit breaker and digital oscilloscope (Explorer II, Nicolet Instruments) a few minutes after the current density had been adjusted. Corresponding values of the hydrogen and oxygen overvoltage, η_{H_2} and η_{O_2} respectively, were calculated from the *IR*-free potential differences, E_c or E_a, with the aid of the following relations:

$$\eta_{H_2} = E_c + 905\,mV \quad (3)$$

and

$$\eta_{O_2} = E_a - 264\,mV \quad (4)$$

In the constants of Equations 3 and 4, the experimentally determined potential difference between the two Hg/HgO (10 M KOH) reference electrodes is taken into consideration, of which one was kept at 100° C and the other at 25° C.

The 10 M KOH solution used was prepared from KOH p.a. (Merck) and deionized water. After a week the solution was replaced with a fresh amount.

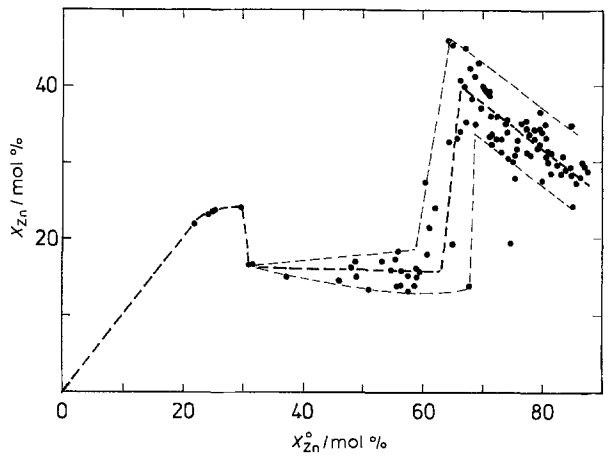

Fig. 1. Plot of the residual zinc content, X_{Zn} (in mol %), in leached alloy against the original zinc content, X_{Zn}^0.

3. Results and discussion

3.1. *Leaching (activation)*

Figure 1 shows the residual zinc content (X_{Zn} in mol %) in leached alloy as a function of the original zinc content, X_{Zn}^0. Despite the scatter of the results, it can be seen that the alloy with $X_{Zn}^0 = 22$ mol % was not attacked at all by cold or hot 10 M KOH solution in the course of about 24 h. The same was also expected for $X_{Zn}^0 < 22$ mol %, as indicated in Fig. 1 by a dotted line with slope $k = 1.0$. Dissolution of zinc from the alloy can be observed for $X_{Zn}^0 > 22$ mol %. The percentage of zinc content in the leached alloy, X_{Zn}, remained almost constant in the limited range of $30 < X_{Zn}^0 < 60$–65 mol %. With further increase in the original zinc content, an increase in the zinc content in the leached alloy up to a sharp maximum with

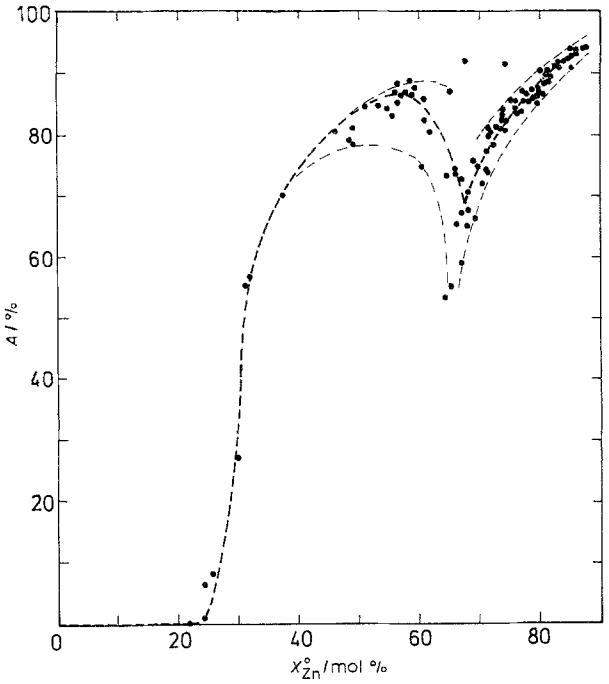

Fig. 2. Plot of the percentage of dissolved zinc, A, against the original zinc content, X^0_{Zn} (in mol %).

approximately X_{Zn} = 35–45 mol % followed by a continuous decrease of this quantity was observed (see Fig. 1).

The percentage of dissolved zinc, A%, is plotted in Fig. 2 as a function of the original zinc content, X^0_{Zn}. The conversion of the primary measurement results was based on the relation

$$A = 100(P_1 - P_2)/P_1 \qquad (5)$$

with $P_1 = X^0_{Zn}/(100 - X^0_{Zn})$ and $P_2 = X_{Zn}/(100 - X_{Zn})$. As can be seen from this diagram, a maximum with A = 82–90% for X^0_{Zn} = 55–58 mol % is observed after the sharp rise of the A fraction in the region of X^0_{Zn} = 22–40 mol %. The dissolved fraction decreases further with increasing X^0_{Zn} until it reaches a sharp minimum with A = 52–65% for X^0_{Zn} = 65–69 mol % and then rises again approaching asymptotically the value $A \to 100\%$ for $X^0_{Zn} \to 100$ mol %.

It was assumed that the discontinuous course of X_{Zn} and A in Figs 1 and 2 as a function of the original zinc content may be related to the structural changes of the alloys. Crystallographic investigations of electrodeposited Ni–Zn alloys carried out so far, for example [8, 9], have shown that the phase spectrum of these alloys is much simpler as compared to the phase spectrum of thermally equilibrated Ni–Zn alloys [10]. Nevertheless, the existence regions of individual phases and phase mixtures of electrodeposited Ni–Zn alloys show rather large differences caused by different electrodeposition conditions used by individual authors.

As X-ray diffraction spectra of our samples were too diffuse for an unambiguous evaluation, rough information about the phase composition of original Ni–Zn alloys was deduced from the results of rest potential measurements given in Fig. 3, simul-

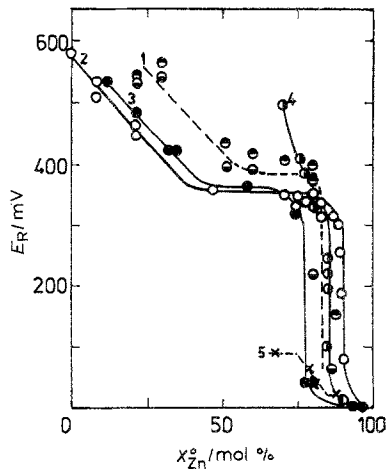

Fig. 3. Plot of rest potential E_R against X^0_{Zn} for electrodeposited (1–4) and thermic (5) Ni–Zn alloys. 1: own results at 25 (◓) and 40° C (◒); 2: (○) [11]; 3: (●) [12]; 4: (◑) [13]; 5: (×) [17]; (◐) [14].

taneously with results of other authors [7, 11–14]. Despite data scattering, a qualitative agreement may be observed between the individual authors' results. A practically linear decrease of E_R for lower X^0_{Zn} values characterizing a single-phase region of the solid solution of zinc in the nickel matrix (α-phase) (curve 1) extends to about 60 mol %. A horizontal part in the region of 50–60 < X^0_{Zn} < 70–80 mol % is indicative of the co-existence of two solid phases (i.e. α + γ) with different proportion. A vertical part of individual curves is characteristic of a single γ-phase capable of existing within a narrow concentration range.

A comparison of the changes in composition of electrodeposited Ni–Zn alloys during leaching in 10 M KOH (Figs 1 and 2) with changes in the rest potential as a function of X^0_{Zn} may lead to the conclusion that the peak of the dissolved zinc fraction A for X^0_{Zn} = 55–58 mol % corresponds to the maximum zinc concentration in the α-phase. A decrease of the dissolved fraction with a sharp minimum at X^0_{Zn} = 65–69 mol % can be attributed to the two-phase mixture α + γ.

Only finding that the zinc dissolution from alloys with $X^0_{Zn} \leqslant 22$ mol % did not take place at all and that a sharp break occurred at X^0_{Zn} = 22 mol % in Figs 1 and 2 seems to be inconsistent with the monotonic almost linear decrease of E_R with increasing X^0_{Zn} in the entire α-phase region. However, the true reason is not an eventual change in the crystallographic structure not identified by rest potential measurements, but a substantially reduced thermodynamic activity of zinc in the solid solutions of the α-phase. Under the simplifying assumption that the measured rest potentials are nearly equal to the equilibrium values, it was calculated that the equilibrium molality of the $Zn(OH)_4^{2-}$ ion during the dissolution of electrodeposited Ni–Zn alloy with X^0_{Zn} = 22 mol % in 10 M KOH at 25° C lies in the range of 10^{-5}–10^{-6} mol kg^{-1}. As can be seen, this value is negligibly low, which indicates that alloy corrosion is negligible. Relevant calculations for 120° C could not be carried out, as the necessary data are not known. However, the results for 25° C can be

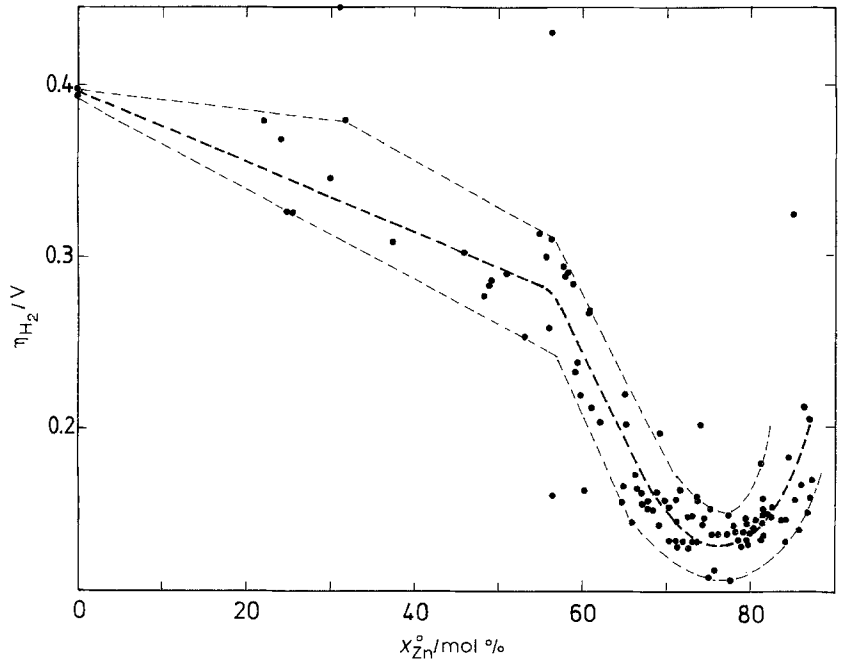

Fig. 4. Plot of the hydrogen overvoltage η_{H_2} at $j_c = 0.4\,A\,cm^{-2}$ in 10 M KOH at 100° C and ambient pressure against zinc content in the raw Ni–Zn alloy.

regarded as clear proof that the negligibly low corrosion of Ni–Zn alloys with $X^0_{Zn} \leqslant 22$ mol % in 10 M KOH found experimentally at temperatures up to 120° C are in full agreement with thermodynamic considerations. Furthermore, in reality, some hydrogen overvoltage must be overcome on the corroding electrode, so that in cases when the reaction Gibbs energy under given conditions is slightly negative, the resulting corrosion rate may be negligibly low.

3.2. *Hydrogen and oxygen overvoltage*

A total of 130 electrode specimens were examined in the manner described. In evaluating the measured results, it became apparent that the dependence of the overvoltage on the current density cannot be expressed by the Tafel relation in all cases. For this reason the hydrogen or oxygen overvoltage at a constant current density $j = 0.400\,A\,cm^{-2}$ (cathodic or anodic) was selected as a quantitative measure of the electrocatalytic activity of the given electrode specimen. This also corresponds to normal operating conditions for advanced alkaline water electrolysis [15].

The dependence of the hydrogen overvoltage η_{H_2} at $j_c = 0.400\,A\,cm^{-2}$ in 10 M KOH at 100° C and ambient pressure on the original zinc content X^0_{Zn} is shown in Fig. 4. Figure 5 shows an analogous dependence for the oxygen overvoltage η_{O_2} at $j_a = 0.400\,A\,cm^{-2}$ under otherwise identical conditions. As can be seen from the two figures, the dependences η_{H_2} and η_{O_2} on X^0_{Zn} display a similar form.

With increasing zinc content in the original electrodeposited Ni–Zn layer in the range $0 < X^0_{Zn} < \sim 57$ mol %, the hydrogen overvoltage dropped roughly linearly from the value for the pure nickel electrode with a slope of $(d\eta_{H_2}/dX^0_{Zn}) = 0.2 \pm 0.05\,mV\,(mol\,\%)^{-1}$. With further increasing zinc content in the original electrodeposited layer, the hydrogen overvoltage dropped much more steeply to a clear minimum at $X^0_{Zn} = 75$–78 mol % where the hydrogen overvoltage ranged between -105 to -145 mV. After this minimum the hydrogen overvoltage rose again fairly steeply with a further increase in the zinc content to that at $X^0_{Zn} = 88$ mol % it reached a value of -170 to -220 mV.

In contrast to the hydrogen overvoltage, the oxygen overvoltage remained practically unchanged in the range $0 < X^0_{Zn} < \sim 57$ mol % (see Fig. 5). However, with a further increase in zinc content it dropped to a minimum at $X^0 = 74$–78 mol % with $\eta_{O_2} = 205$–255 mV. After this a clear rise in the oxygen overvoltage was again observed with a further increase in the zinc content X^0_{Zn}. As can be seen from the two figures, the overvoltage minimum for both electrode reactions appears at the same composition of the original electrodeposited layer, i.e. at $X^0_{Zn} = 74$–68 mol %. This composition corresponds to the pure γ-phase, as deduced from Fig. 3. An approximately linear decrease of the hydrogen overvoltage or approximately constant oxygen overvoltage in the range $0 < X^0_{Zn} < 50$–60 mol % corresponds to the α-phase region in the original Ni–Zn alloys. The steeper decrease of the hydrogen, as well as oxygen, overvoltage in the range of about $50\text{–}60 < X^0_{Zn} < 74$ mol % corresponds to the phase mixture $\alpha + \gamma$, with successively increasing fraction of the γ-phase in the original alloy, leading to more active layers after leaching. A significant increase in the overvoltage of both electrode reactions on electrodes prepared by leaching electrodeposited Ni–Zn layers with $X^0_{Zn} > 78$ mol % may be ascribed to the increasing amount of other phase(s) (denoted as δ and η) in the mixture with the γ-phase [9] leading to very low active layers after leaching.

It can therefore be concluded that highly active

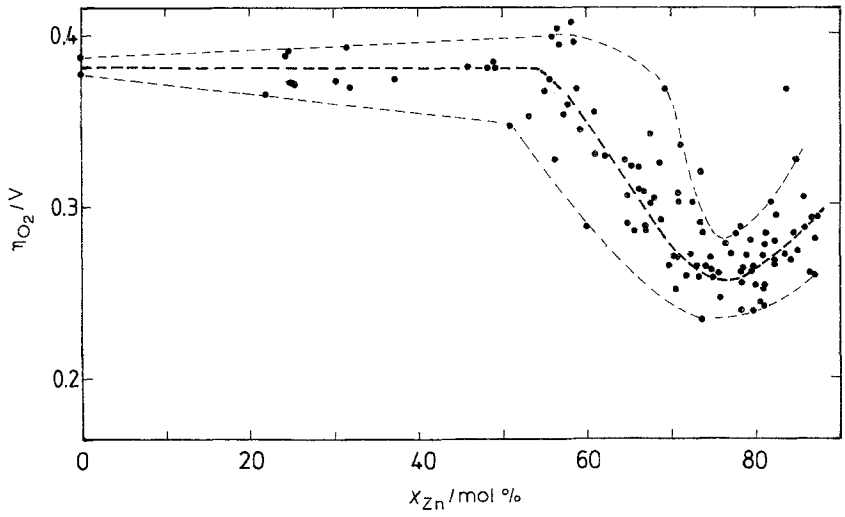

Fig. 5. Plot of the oxygen overvoltage η_{O_2} at $j_a = 0.4\,A\,cm^{-2}$ in 10 M KOH at 100° C and ambient pressure against zinc content in the raw Ni–Zn alloy.

Raney nickel electrodes on Ni–Zn base for hydrogen and also oxygen evolution from alkaline solutions can be fabricated from electrodeposited Ni–Zn layers with X^0_{Zn} = 74–78 mol %, corresponding to pure γ-phase. This conclusion is in good agreement with previous findings [3, 4].

No interrelations between the hydrogen and oxygen overvoltage and the true surface area of Raney nickel electrodes on Ni–Zn base were investigated in this study. From a previous paper [16], however, it followed that a direct proportionality exists between the hydrogen overvoltage on such electrodes and their specific area.

An interesting conclusion may be made from the plot of hydrogen and oxygen overvoltage against the residual zinc content X_{Zn} in the activated electrodeposited layer (see Figs 6 and 7). Despite the wide scatter, clear overvoltage minima may be observed in both cases at a residual content of X_{Zn} = 32–34 mol %.

If this optimum residual content is reduced in the course of long-time operation, particularly in the case of discontinuous current load, this may result in a decrease in the electrocatalytic activity of such electrodes [17].

The wide scatter of data in all figures is attributable to the fact that the original zinc content X^0_{Zn} was regarded as the only parameter in these evaluations without taking into consideration the changes in other co-determining parameters. Since, however, a Ni–Zn alloy of given composition can be prepared under various deposition conditions (current density, temperature, composition and pH of the bath) it is quite understandable that the Ni–Zn alloys of the same composition may differ in individual physico-chemical properties. Therefore, not all Raney nickel electrodes on the Ni–Zn base prepared by leaching the alloy with an optimum composition of X^0_{Zn} = 74–78 mol % (deposited under arbitrary conditions) have the lowest possible hydrogen and oxygen overvoltage.

The knowledge of the optimum operating conditions for the electrodeposition of Ni–Zn alloys, as precursors for highly active Raney nickel electrodes for hydrogen and oxygen evolution from alkaline solutions, is extremely important operating information.

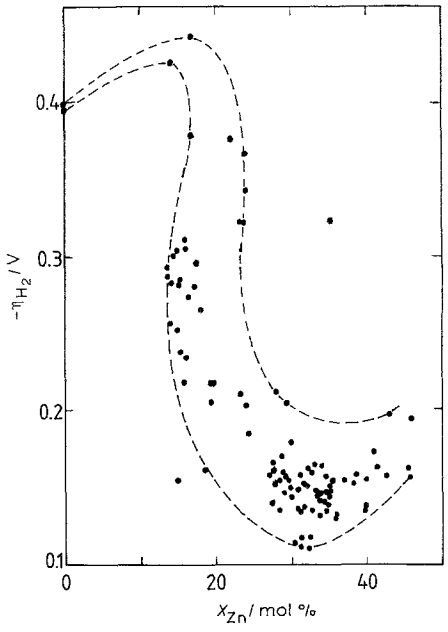

Fig. 6. Plot of the hydrogen overvoltage η_{H_2} against residual zinc content X_{Zn} in the activated Ni–Zn electrodeposited layer.

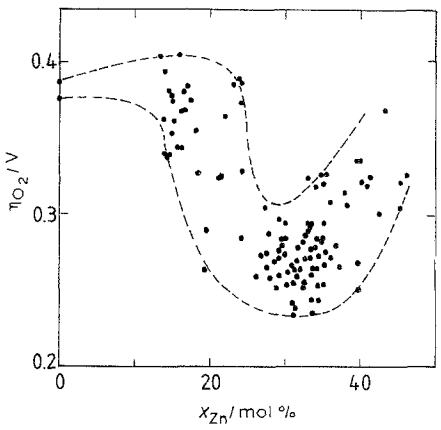

Fig. 7. Plot of the oxygen overvoltage η_{O_2} against residual zinc content X_{Zn} in the activated Ni–Zn electrodeposited layer.

References

[1] J. Balej, J. Divisek, H. Schmitz and J. Mergel, *J. Appl. Electrochem.* **22** (1992).
[2] Y. Choquette, L. Brossard and H. Ménard, *ibid.* **20** (1990) 855.
[3] K. Sasaki and K. Sugiyama, *Kogyo Kogaku Zasschi* **60** (1957) 387.
[4] I. Paseka and J. Balej, *Chem. prům.* **20** (1970) 305.
[5] J. Balej, *Int. J. Hydrogen Energy* **10** (1985) 89.
[6] J. Divisek, H. Schmitz and J. Balej, *J. Appl. Electrochem.* **19** (1989) 519.
[7] G. Schwitzgebel, J. Lang and R. Sass, *Z. Phys. Chem. (N.F.)* **146** (1985) 87.
[8] A. Brenner, 'Electrodeposition of Alloys', Vol. II, Academic Press, New York (1963) pp. 194–238.
[9] D. E. Hall, *Plat. Surf. Finish.* **70** (1983) 59.
[10] M. Hansen and K. Anderko, 'Constitution of Binary Alloys', 2nd Ed., McGraw-Hill, New York (1958) p. 1060.
[11] A. Imai, T. Watanabe and M. Kurachi, *Denki Kagaku* **46** (1978) 202.
[12] E. P. Schoch and A. Hirsch, *Trans. Electrochem. Soc.* **11** (1907) 135.
[13] N. T. Kudryavtsev, T. G. Smirnova and O. P. Volkova, *Prot. Met.* **2** (1966) 597.
[14] P. M. Vyacheslavov, G. B. Kabanov, M. M. Bodyagina and A. O. Bodyagin, *J. Appl. Chem. (USSR)* **57** (1984) 1191.
[15] J. Divisek, Water electrolysis in a low- and medium-temperature regime, in 'Electrochemical Hydrogen Technologies. Electrochemical Production and Combustion of Hydrogen' (edited by H. Wendt), Elsevier, Amsterdam (1990) pp. 137–212.
[16] J. Divisek, J. Mergel and H. Schmitz, *Int. J. Hydrogen Energy* **7** (1982) 695.
[17] J. Divisek, J. Mergel and H. Schmitz, *ibid.* **15** (1990) 105.